International Journal of Bifurcation and Chaos, Vol. 11, No. 6 (2001) 1771–1779

TIME AVERAGING OF IRREGULAR SPATIOTEMPORAL PATTERNS OF A LARGE APERTURE LASER IN TRANSITORY REGIME

F. ENCINAS-SANZ, I. LEYVA* and J. M. GUERRA
Departameuto de Optica, Facultad de CC. Físicas,
Universidad Complutense de Madrid 28040 Madrid, Spain

Received May 23, 2000; Revised October 12, 2000

By means of a new experimental technique, we measure quasi-intantaneous transverse intensity patterns in the gain-switch peak of a transversely excited atmospheric CO_2 laser with large aperture. The patterns recorded with a 2 ns resolution show a completely irregular spatiotemporal behavior, but when the exposure time of the measurements increases, boundary-determined ordered structures can be observed. As a quantification of this averaging process, the contrast of the intensity distributions decreases as the time integration grows. The results are numerically reproduced by integration of the full Maxwell–Bloch equations.

1. Introduction

Pattern formation in nonlinear systems has attracted much interest in last years. When the aspect ratio is small, the behavior of the system can be explained in relation to the influence of the boundary conditions, such as modal dynamics in optical systems. But as the transverse size increases, the behavior becomes more and more boundary-independent. In this case, the structure formation begins to be dominated by the bulk parameters and nonlinearities of the medium, and then turbulence and defects arise spontaneously.

However, between both extreme and ideal behaviors — purely boundary selected or completely boundary free — the dynamics of real systems is more likely to present a whole range of intermediate behaviors including features of both regimes. In particular, averaging processes from chaotic to boundary-selected ordered patterns have been observed in extended systems such as hydrodynamic Faraday waves [Gluckman *et al.*, 1993], rotating thermal convection [Ning *et al.*, 1993] or electroconvection [Rudroff & Rehberg, 1997]. In these works, large aspect ratio systems exhibiting spatiotemporal chaos in instantaneous recording, let us see the underlying boundary-determined order when examined over a sufficiently long time.

Taking into account the striking universality of these processes, a similar behavior is foreseeable in large aperture optical systems, and so has been predicted from the basis of the Maxwell–Bloch [Huyet *et al.*, 1995; Huyet & Tredicce, 1996; Feng *et al.*, 1993; Staliunas & Weiss, 1995; Harkness *et al.*, 1994] and Kuramoto–Sivashinsky [Huyet & Tredicce, 1996; Eguiluz *et al.*, 1999] equations.

On the experimental side, it has to be considered that the observation of this long term order recovering requires the ability to measure both instantaneous and averaged patterns. This has been possible in systems with a slow dynamics as photorefractive oscillators [Farjas *et al.*, 1994]. However, although much interesting experimental work has been carried out in large aperture lasers unfortunately, the extremely fast evolution (characteristic times of some nanoseconds for CO_2 lasers,

*E-mail: ileyva@eucmos.sim.ucm.es

and picoseconds for semiconductor laser) makes the experimental problem of the time resolved recording of large aperture laser patterns to remain unsolved so far [Huyet *et al.*, 1995; Huyet & Tredicce, 1996; Dangoisse *et al.*, 1992; Louvergneaux *et al.*, 1996; Labate *et al.*, 1997; Fisher *et al.*, 1993; Hegarty *et al.*, 1999].

Our group has removed partially this limitation thanks to the development of an experimental set-up which allow us to record instantaneous transverse patterns on the nanosecond time scale. Thus we have been able to study, both experimentally and theoretically, the time resolved spatiotemporal dynamics of a transversely excited atmospheric (TEA) CO_2 pulsed laser with a relatively large Fresnel number [Encinas-Sanz *et al.*, 2000], when operating in the long pulse regime (about 2 μs). This time length turns out to be more than a magnitude order longer than the smaller time constant of the system, which in our laser is the population life time $\gamma_{\parallel}^{-1} \simeq 10^{-7}$ s. Therefore, in this regime the dynamics can be consider as quasi-stationary.

However, this laser can also be operated in a short pulse regime (gain-switch pulse width $\simeq 10^{-7}$ s), which cannot be considered as quasi-stationary any longer, but is just a purely transitory regime. This is rarely considered in the general studies of laser dynamics, even though the pulsed operation is the commonest in many real lasers, especially in those with large apertures. In this work we show that even this fully transient dynamics displays features of spatiotemporal turbulence with an underlying order on time average. In Sec. 2 we detail the experimental setup. Section 3 contains the experimental results of this work, which are numerically reproduced in Sec. 4. Finally, we extract some conclusions in Sec. 5.

2. Experimental Setup

A half-symmetric resonator has been used in our TEA CO_2 laser, and a distance $L = 112$ cm separates the concave ($r = 10$ m) and plane mirrors [Encinas-Sanz & Guerra, 1990]. The separation between the transverse electrodes may be taken as the laser aperture ($2b \simeq 20$ mm) yielding to a Fresnel number of

$$F = \frac{b^2}{L\lambda} \simeq 10\,. \tag{1}$$

An intracavity Brewster plate produces a very good polarization in the laser beam. The gas laser mixture has no N_2, in order to limit the output to the gain-switch pulse with a width of about 100 ns. The laser pulse propagates across a Pockels electrooptic cell arriving to a custom-made high quality polarizer crossed with laser polarization (Fig. 1). This polarizer partially rejects the light pulse to a laser triggered spark-gap, which once fired generates a high voltage pulse ($V_\pi = 8.48$ kV), that travels to the electrooptic CdTe crystal, generating a transverse Pockels effect. This causes the polarization of the linearly polarized laser beam to turn by 90°, which can now be transmitted by the polarizer as long as the high-voltage pulse lasts, and so we finally obtain a time slice of the laser pulse. The voltage pulse duration, and therefore the slice width, is controlled by the length of the coaxial pulse forming a line that links the spark gap and the high-voltage charge resistor. Likewise, the relative position of the time slice within the laser pulse depends on the length of the delay cable that links the spark gap and the switching device. The high extinction ratio of the polarizer allows for a very small energy background transmission during the whole laser pulse; otherwise, the instantaneous pattern could be blurred and the information lost. To avoid diffraction in the aperture of the Pockels cell, a telescopic system placed at the beam exit reduces its transverse size. Once the selfsyncrhonized electrooptic shutter is opened, the transmitted time slice of the laser pulse reaches the pyroelectric bidimensional array of a computer controlled camera (0.1 mm spatial resolution).

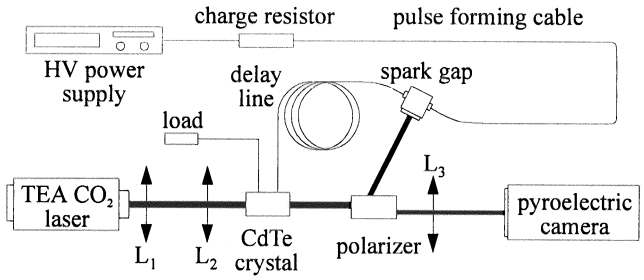

Fig. 1. Experimental setup.

3. Experimental Results

Before beginning the pattern morphogenesis picture, the temporal evolution of the short laser pulses has to be studied, in order to know the time scales involved in the dynamics. The measurements were performed by a rapid ($\simeq 1$ ns rise time)

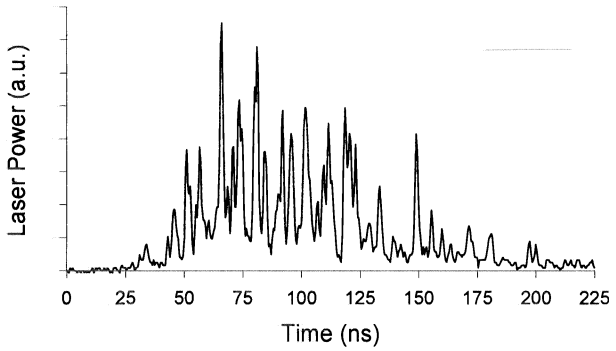

(a)

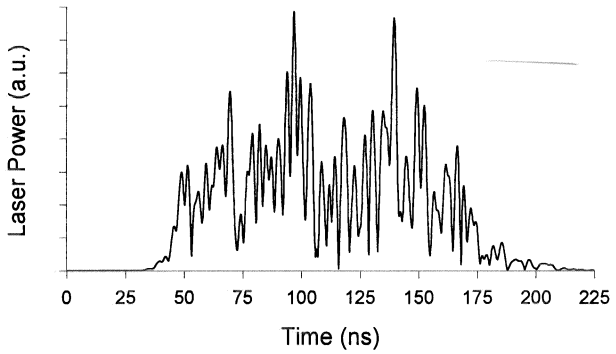

(b)

Fig. 2. Local intensity temporal evolution of the laser pulse: (a) experimental, (b) numericaly generated for $r_{\max} = 70$, $\delta = 0.25$.

photon drag detector linked to a 600 MHz and 2 Gigasamples/s real time digitizer placed in a Faraday cage. The local intensity of the laser pattern was measured through a small pinhole with diameter $\simeq 1$ mm. We find a strongly irregular local intensity [Fig. 2(a)] with a characteristic period of a few nanoseconds ($\simeq 6$ ns).

Once we know the temporal characteristics of the emission, we are ready to investigate the spatial ones. Almost instantaneous (2 ns time slice width) transverse intensity distributions, can be registered and stored by means of the setup described above. Figure 3 shows a sample of the measured patterns taken for different laser shots with a 2 ns time window width at the same temporal position, corresponding with a time delay of 75 ns measured from the peak of the gain-switch pulse [Fig. 4(a)]. It can be seen that the instantaneous patterns are highly irregular. The positions at which the laser intensity maxima appear are different in all the registered instantaneous patterns, i.e. shot to shot the instantaneous intensity distributions are not reproducible.

We want to know if the pattern appearance is irregular all along the laser pulse. For this purpose we repeat the measurements shown in Fig. 3, but now centered on the maximum of the gain-switch pulse [Figs. 4(b), 5(a) and 5(b)]. As in the previous case (75 ns delay), the overall appearance is very disordered, showing a deep spatial modulation with a small number of local maxima. This observation suggests that the intensity distribution keeps on being irregular throughout the whole 100 ns of the pulse.

To complete the description of the dynamics, one might wonder whether this instantaneous transverse intensity distribution remains static or evolves, changing throughout the pulse duration. The most straightforward way to test this possibility would be to take consecutive instantaneous snapshot along a single pulse. However, our setup cannot be operated in this repetitive way. As an alternative, the patterns in different laser pulses were measured taking time slices with increasing duration. In particular, temporal slices of 2, 3, 6, 10, 30, 60 ns and the full gain-swith were recorded. Some of the corresponding patterns appear in Fig. 6. It can be concluded that the instantaneous pattern, keeping its irregular character, changes along the pulse, since more and more local intensity maxima appear in the progressively time integrated measurements. In addition, it is clear that the position of the new maxima is not completely random: the disordered structure observed in the short exposure time images [Fig. 6(a)], yields to progressively more ordered intensity distributions, uncovering the boundary-determined symmetry. Therefore, the spatial order manifest even in this turbulent nonstationary evolution which, as a whole, is no longer than 30 times the intensity fluctuation period (Fig. 2), [Encinas-Sanz *et al.*, 2000].

We can have another insight to this integration process in the Fourier plane. On one hand, the power spectra of instantaneous patterns are irregular, almost unstructured and not reproducible from shot to shot [Fig. 7(a)]. On the other hand, in the average of the spectra of one hundred instantaneous patterns, two well defined maxima can be observed [Fig. 7(c)]. As has been observed in previous studies, this also means the existence of a hidden regularity, which may be uncovered by averaging over many instantaneous patterns [Encinas-Sanz *et al.*, 1996]. Thus the average pattern is ordered showing the typical fringes that are found in the long pulse (quasi-stationary) time integrated

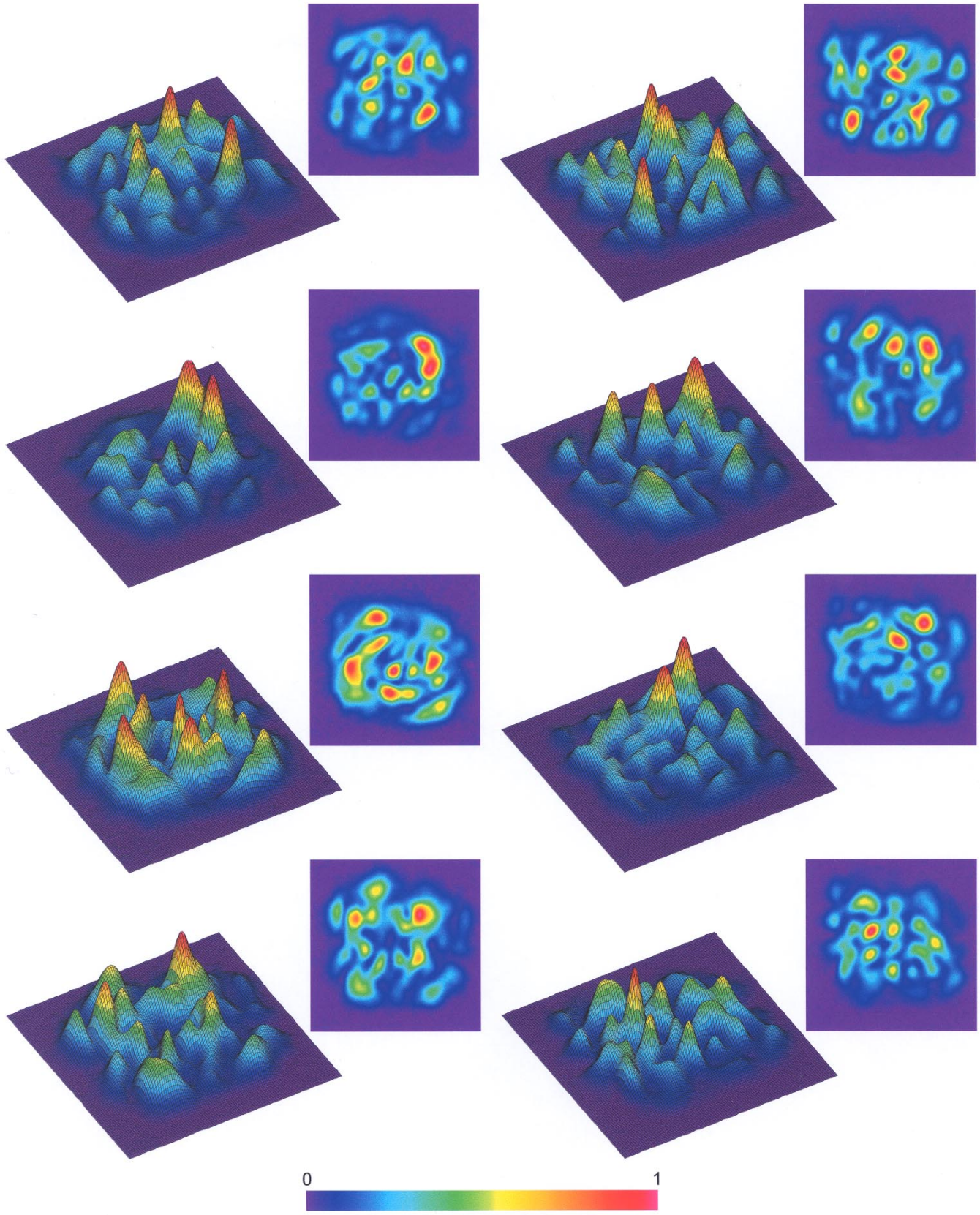

Fig. 3. Instantaneous patterns taken at different pulses with a time slice width of 2 ns and delay time of 75 ns measured from the gain-switch peak of the pulse. Real pattern dimension $\simeq 20 \times 20$ mm. The color-bar used in the figures is included.

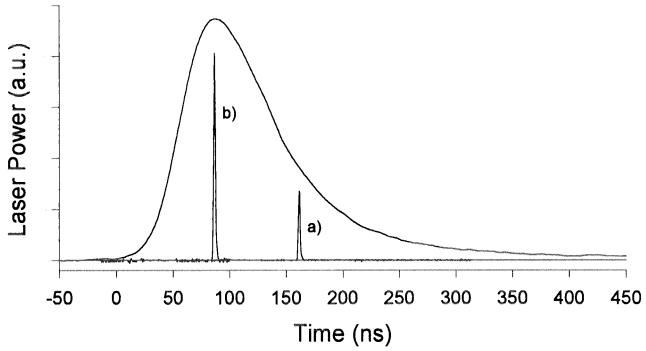

Fig. 4. Two time slices synchronized with the whole gain-switch pulse: (a) near the peak, (b) 75 ns after. Slice duration: 2 ns.

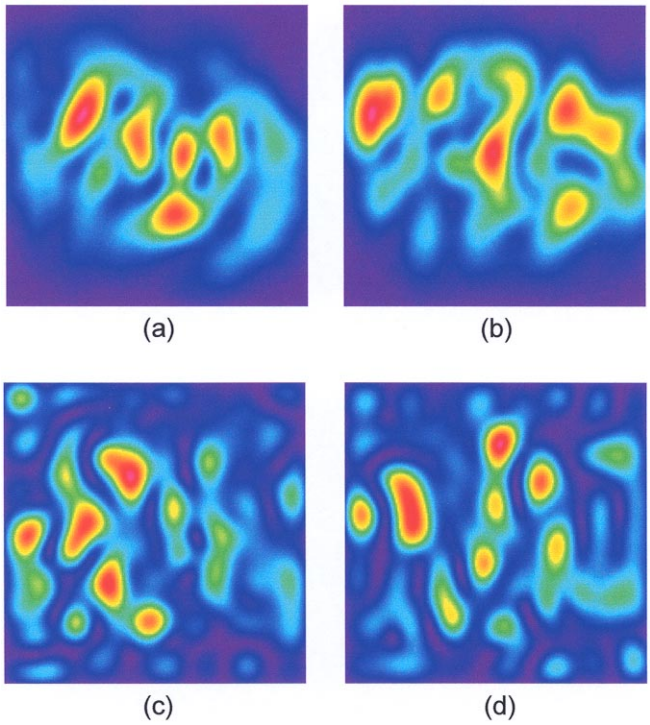

Fig. 5. Instantaneous patterns (2 ns time slice): (a) and (b) experimental, (c) and (d) numerically generated counterparts.

patterns [Encinas-Sanz *et al.*, 2000; Hegarty *et al.*, 1999].

In addition, at first glance it is possible to observe how the contrast between the intensity peaks and valleys decreases when the time integration interval is elonged. If we calculate the average of the intensity distribution across the surface of the pattern I_m, a measurement of the contrast C in the patterns may be found by the relationship between the peak maximum I_p above the average I_m and the average itself

$$C = \frac{I_p - I_m}{I_m}\,. \tag{2}$$

For each measured integration time Δt considered in Fig. 6, the contrasts of one hundred patterns were averaged to get a meaningful value of C. The contrast C as a function of the temporal slice duration Δt is shown in Fig. 8. An hyperbolic functional form

$$C(\Delta t)^{n_e} = \alpha \tag{3}$$

fits well to the experimental data [Fig. 8(a)], where $n_e = 0.36 \pm 0.02$, α is a normalization constant and Δt is given in seconds. This contrast accounts for the integration of a growing number of local intensity maxima scattered across the pattern as the temporal window is made longer (Fig. 6), and can be considered a representative parameter to quantify the turbulent dynamics and its averaging process.

4. The Model and Theoretical Results

In order to compare our observations with the class B laser semiclassical theory, and thus try to reproduce the measured spatiotemporal dynamics, we directly integrate the two-level Maxwell–Bloch equations [Huyet & Rica, 1996]:

$$\frac{\partial E}{\partial t} = -\kappa\left[(1 - i\delta) - i\frac{a}{2}\Delta_t\right]E - \kappa r P\,, \tag{4}$$

$$\frac{\partial P}{\partial t} = -\gamma_\perp[DE + (1 + i\delta)P]\,, \tag{5}$$

$$\frac{\partial D}{\partial t} = -\gamma_\parallel\left[D - 1 - \frac{1}{2}(EP^* + E^*P)\right]\,, \tag{6}$$

where $E = E(\mathbf{x}, t)$ is the slowly varying electric field, $P = P(\mathbf{x}, t)$ the polarization, $D = D(\mathbf{x}, t)$ the population inversion, $r = r(\mathbf{x}, t)$ the rescaled pump, κ represents the cavity losses, $a = c\lambda/2\pi\kappa b^2$ is a diffraction coefficient, and $\delta = \omega_{21} - \omega/\gamma_\perp + \kappa$ the rescaled detuning, where ω_{21} is the frequency of the transition and ω is the frequency of the laser emission. Likewise, Δ_t is the Laplacian in the dimensional transverse coordinates of the system $\mathbf{x} = (x, y)$. In an atmospheric laser, the polarization decay rate can be chosen as $\gamma_\perp = 3 \times 10^9$ s^{-1} and the inversion decay rate as $\gamma_\parallel = 10^7$ s^{-1}. We take the losses coefficient as $\kappa = 9.0 \times 10^7$ s^{-1}.

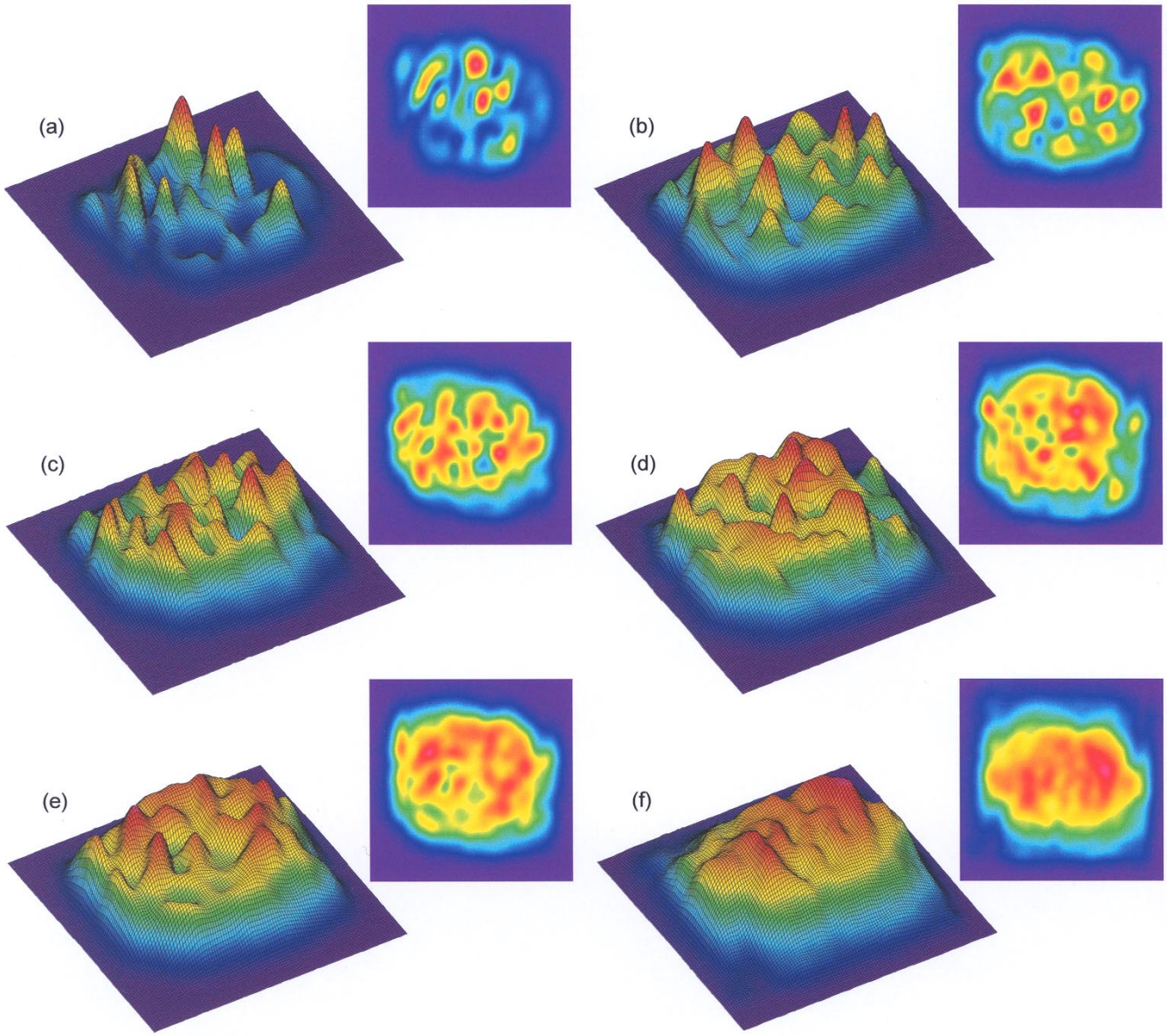

Fig. 6. Time integrated patterns recorded with different temporal slice widths: (a) 2 ns, (b) 6 ns, (c) 11 ns, (d) 30 ns, (e) 60 ns, (f) the full gain-switch pulse.

The transverse pumping profile is taken to be homogeneously distributed along one transverse axis and Gaussian in the other, in order to reproduce the experimental current spatial distribution of the glow discharge that pumps the laser. Likewise, we simulate the temporal form of the pumping by a cosenoidal function approaching the pulsed excitation, with large pumping parameters in the maximum ($r_{\max} \simeq 60 - 70$) and about 100 ns width, as in the real laser. To simulate the spontaneous emission, which is not considered in the semiclassical treatment, a weak white noise is used as initial condition for the fields.

A null boundary condition is used, which keeps the electric field as zero at the edges of the laser aperture. This realistic boundary condition differs from the periodic boundary usually used in the simulation of extended nonlinear systems. However, we observe that it plays an essential role in the reproduction of the experiment, and particularly, in the averaging to order [Harkness *et al.*, 1994; Encinas-Sanz *et al.*, 2000; Eguiluz *et al.*, 1999].

With such a simple model, we have reproduced most of the main features of our observations. Thus, local intensity temporal evolution and the patterns

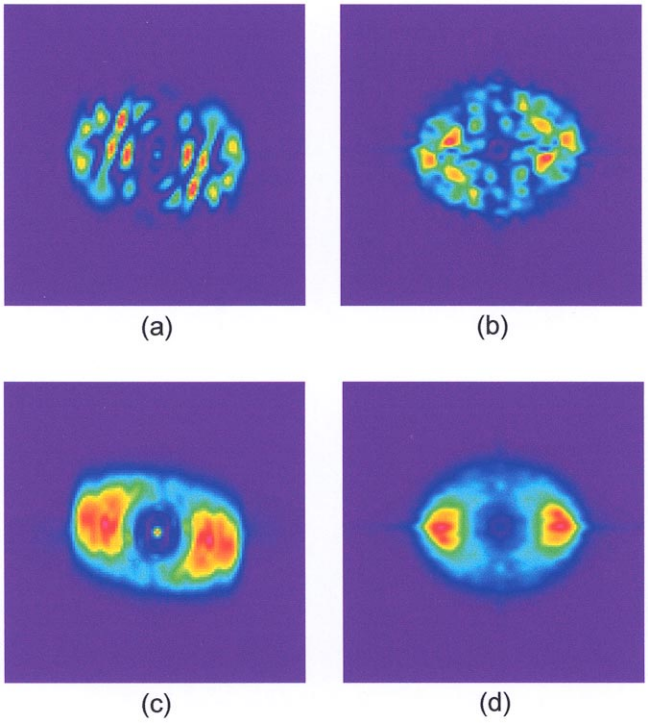

Fig. 7. Spatial Fourier spectra of one (a) experimental, (b) numerical instantaneous pattern. Average of the spatial fourier spectra of (b) one hundred experimental instantaneuos patterns, (d) fifty numerical intantaneous patterns.

obtained by a standard numerical method, look very similar to those recorded experimentally.

The local temporal evolution of the intensity obtained by numerical simulation is completely irregular [Fig. 2(b)], showing the same pulse length and characteristic fluctuation time than its experimental counterpart [Fig. 2(a)]. In the spatial domain, the instantaneous patterns are well reproduced as can be seen in Fig. 5, in which a pair of experimental patterns [Figs. 5(a) and 5(b)] are compared with the equivalent numerically generated ones [Figs. 5(c) and 5(d)]. These are also completely disordered and nonreproducible, showing several maxima randomly distributed with an equivalent size of about 1.5 mm, which perfectly agrees with the experimental observation.

This can be also seen in the Fourier domain, where the results reproduce the experiment, both for the power spectra of the single instantaneous patterns [Fig. 7(b)] and the averaged over fifty samples [Fig. 7(d)]. This proves the essential role of the boundary condition in the selection of the pattern.

We have also reproduced the experiment for the progressively integrated patterns, previously shown in Fig. 6. Figure 9 shows the corresponding

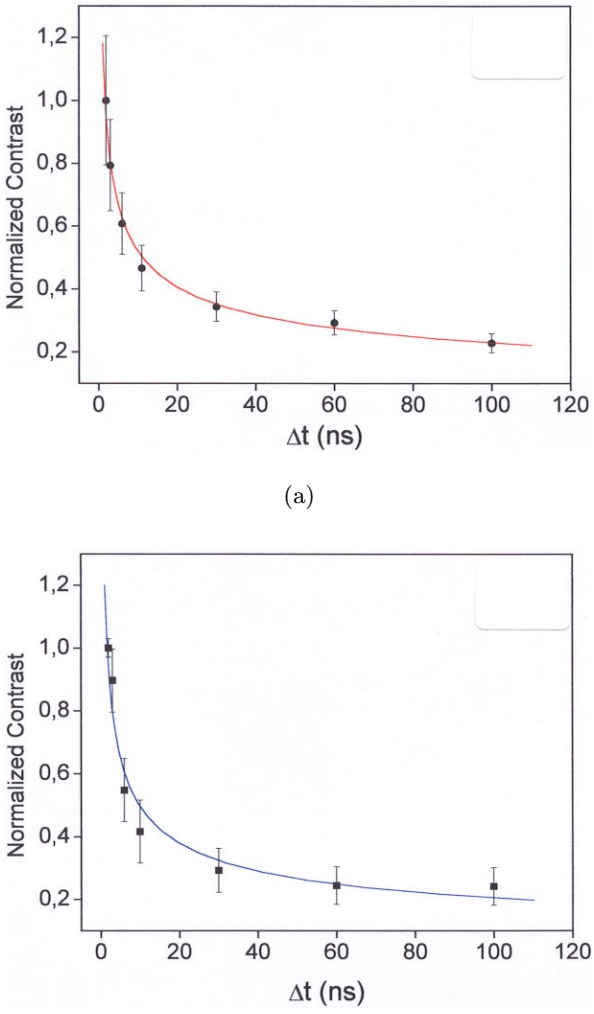

Fig. 8. Pattern contrast as a function of the time slice width: (a) experimental, (b) numerically generated.

theoretical time integrated patterns for exposures of 2, 6, 10, 30, 60 and 100 ns [Figs. 9(a)–9(f), respectively], where the outstanding agreement with their experimental counterparts can be seen, following the same evolution from turbulent behavior to boundary selected order. Likewise, the loss of contrast of this progressively integrated patterns, calculated as in the experimental case, can also be approximated by an equivalent hyperbolic function $C(\Delta t)^{n_t} = \alpha'$. The contrast of fifty numerical patterns for each value of Δt were averaged to get $n_t = 0.38 \pm 0.04$ [Fig. 8(b)], a compatible value with that obtained for the experimental data.

5. Conclusions

In conclusion, we have studied experimentally the time resolved pattern formation in the short

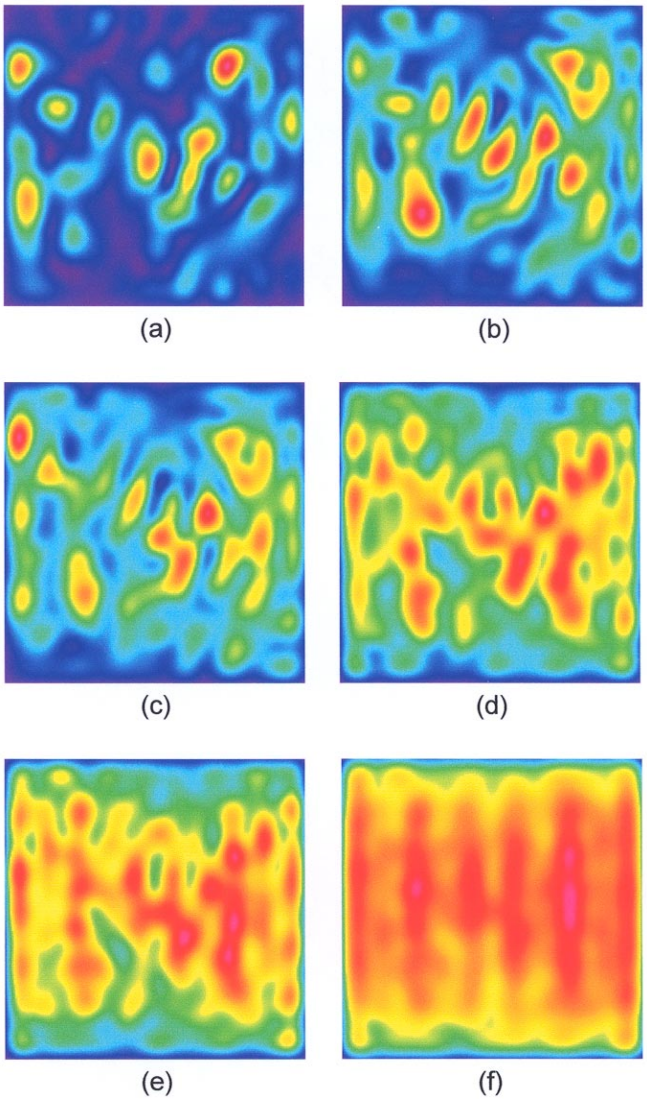

Fig. 9. Numerically generated time integrated patterns recorded with different temporal slices width: (a) 2 ns, (b) 6 ns, (c) 10 ns, (d) 30 ns, (e) 60 ns, (f) the full gain-switch pulse.

gain-switch pulse of a TEA CO_2 laser with a relatively large Fresnel number. As in the quasi-stationary case [Encinas-Sanz *et al.*, 2000], an irregular spatiotemporal dynamics is observed even in this transient laser regime. The instantaneous pattern consists of a group of irregularly distributed maxima, which evolves in a complicated way, retaining the nonordered appearance along the pulse. As it has been observed in much other pattern forming systems, this turbulence yields to boundary-determined order on average, when progressively time integrated patterns are recorded. In addition, during this time integration the contrast of the patterns decays monotonically, which in some way allows us to quantificate the averaging process. All these experimental features are faithfully reproduced by a simple numerical model based on the Maxwell–Bloch equations.

Acknowledgments

The research work leading to this paper has been supported by the Comisión Interministerial de Ciencia y Tecnología of Spain, under Project PB95-0380.

References

Biswas, D. J. & Harrison, R. G. [1986] "Observation of pulsating instabilities and chaos in a transversely excited atmospheric pressure CO_2 laser," *Opt. Commun.* **57**, 193–195.

Dangoise, D., Hennequin, D., Lepers, C., Louvergenaux, E. & Glorieux, P. [1992] "Two dimensional optical lattices in a CO_2 laser," *Phys. Rev.* **A49**, 5955–5958.

Encinas-Sanz, F. & Guerra, J. M. [1990] "A powerful transversely excited multigas laser system," *Meas. Sci. Technol.* **1**, 1188–1192.

Encinas-Sanz, F., Pastor, I. & Guerra, J. M. [1996] "Transverse pattern morphogenesis in a CO_2 laser," *Opt. Lett.* **21**, 1153–1155.

Encinas-Sanz, F., Leyva, I. & Guerra, J. M. [2000] "Time resolved pattern evolution in a large aperture laser," *Phys. Rev. Lett.* **84**, 883–886.

Eguíluz, V. M., Alstrøm, P., Hernández-García, E. & Piro, O. [1999] "Average patterns of spatiotemporal chaos: A boundary effect," *Phys. Rev.* **E59**, 2822–2825.

Farjas, J., Hennequin, D., Dangoisse, D. & Gloriex, P. [1994] "Role of symmetries in the transition to turbulence in optics," *Phys. Rev.* **A57**, 580–584.

Feng, Q., Moloney, J. & Newell, C. [1993] "Amplitude instabilities of transverse traveling waves in lasers," *Phys. Rev. Lett.* **71**, 1705–1708.

Fisher, I., Hess, O., Elsaßer, W. & Gobël, E. [1996] "Complex spatiotemporal dynamics in the near-field of a broad-area semiconductor laser," *Europhys. Lett.* **35**, 579–584.

Gluckman, B. J., Marcq, P., Bridger, J. & Gollub, J. [1993] "Time averaging of chaotic spatiotemporal wave patterns," *Phys. Rev. Lett.* **71**, 2034–2037.

Harkness, G. K., Firth, W. J., Geddes, J. B., Moloney, J. V. & Wright, E. M. [1994] "Boundary effects in a large aspect ratio lasers," *Phys. Rev.* **A50**, 4310–4317.

Hegarty, S. P., Huyet, G. & McInerney, J. G. [1999] "Pattern formation in the transverse section of a laser

with a large Fresnel number," *Phys. Rev. Lett.* **82**, 1434–1437.

Huyet, G., Martinoni, M. C., Tredicce, J. R. & Rica, S. [1995] "Spatiotemporal dynamics of lasers with large Fresnel number," *Phys. Rev. Lett.* **75**, 4027–4030.

Huyet, G. & Rica, S. [1996] "Spatiotemporal instabilities in the transverse pattern of lasers," *Physica* **D96**, 215–229.

Huyet, G. & Tredicce, J. R. [1996] "Spatiotemporal chaos in the transverse section of lasers," *Physica* **D96**, 209–214.

Labate, A., Ciofini, M., Meucci, R., Bocaletti, S. & Arecchi, F. T. [1997] "Pattern dynamics in a large Fresnel number laser close to threshold," *Phys. Rev.* **A56**, 2237–2241.

Louvergenaux, E., Hennequin, D., Dangoise, D. & Glorieux, P. [1996] "Transverse mode competition in a CO_2 laser," *Phys. Rev.* **A53**, 4435–4438.

Ning, L., Hu, Y., Ecke, R. & Ahlers, G. [1993] "Spatial and temporal averages in chaotic patterns," *Phys. Rev. Lett.* **71**, 2216–2219.

Pastor, I., Encinas-Sanz, F. & Guerra, J. M. [1991] "Spatiotemporal instabilities from a transversely excited atmospheric CO_2 laser," *Appl. Phys.* **B52**, 184–190.

Rudroff, S. & Rehberg, I. [1997] "Pattern formation and spatiotemporal chaos in the presence of boundaries," *Phys. Rev.* **E55**, 2742–2749.

Staliunas, K. & Weiss, C. O. [1995] "Nonstationary vortex lattices in large-aperture class B lasers," *J. Opt. Soc.* **B12**, 1142–1149.